The allowed β decay[3,4] going almost exclusively to the 0.425-MeV state indicates that the ground state of Se^{73} would be a single-neutron $g_{9/2}$ configuration, as expected from the shell model. This transition from $g_{9/2}$ neutron to $g_{9/2}$ proton is in keeping with the above data.

ACKNOWLEDGMENTS

The author would like to acknowledge helpful discussions with D. Kurath. He is also indebted to M. Oselka and the cyclotron crew for the several bombardments and to M. Wahlgren for the chemistry facilities provided.

PHYSICAL REVIEW VOLUME 131, NUMBER 2 15 JULY 1963

Capture-Gamma Determination of Chromium-54 Structure

DONALD H. WHITE
Lawrence Radiation Laboratory, University of California, Livermore, California
(Received 11 March 1963)

Gamma emission following thermal-neutron capture in separated chromium-53 has been studied at the Livermore 2-MW pool-type reactor using a fast coincidence scintillation spectrometer. A quartz-crystal thermal-neutron filter is described which produces a flux of 10^6 neutrons/cm^2 sec at the target with a cadmium ratio better than 10^4. Capture gammas are observed at 9.72, 8.88, 7.10, 6.88, 6.64, 6.28, 6.00, 4.86, 3.72, 2.60, 2.24, 2.00, 1.77, and 0.84 MeV. Cascade transitions were studied using coincidence, sum coincidence, and angular correlation methods. A "double-window" coincidence technique used in these measurements is described. This technique systematically subtracts coincident background and is particularly applicable to angular correlation measurements. Energy levels are established at 0.84, 2.61, 2.84, 3.08, 3.44, 3.72, and 4.86. MeV. The spins of the first four excited states are 2, 2, 0, and 2, respectively, as determined by angular correlation and cascade systematics. The results are discussed in terms of recent nuclear models.

I. INTRODUCTION

THE nucleus chromium-54 has two $p_{3/2}$ neutrons and four $f_{7/2}$ protons outside the closed shells. It is in the medium mass region and is particularly amenable to shell-model calculations involving coupling between nucleon groups in different shells.

Energy levels at 4.04, 1.83, and 0.84 MeV have been determined by Schardt and Dropesky[1] from β decay of vanadium-54. The 0.84 level has also been populated by manganese-54 K-capture[2] ($E=0.835\pm0.001$ MeV), by Coulomb excitation[3] ($\tau=1.7\times10^{-11}$ sec), and by inelastic proton scattering.[4] Deuteron stripping measurements were made by Elwyn and Shull[5] using separated Cr^{53} (spin $\frac{3}{2}^-$). They found Cr^{54} levels at 0.86, 1.31, 2.67, 3.19, and 3.79 MeV. El Bedewi and Tadros[6] used deuteron stripping on natural chromium and determined the isotopic contribution by consistency of the calculated Q values at different proton recoil angles. They found Cr^{54} levels at 0.81, 1.23, 2.60, and 3.03 MeV. In both experiments, all proton recoil distributions were characterized by angular momentum $l=1$, restricting the level spins to 0^+, 1^+, 2^+, and 3^+.

Natural chromium capture gammas above 3 MeV have been measured by Kinsey and Bartholomew[7] (hereafter referred to as KB) using a pair spectrometer. Groshev *et al.*[8] (hereafter referred to as GDLP) used a Compton recoil spectrometer to observe capture gammas above 0.5 MeV. Both instruments were especially suited to the high-energy region. The low-energy spectrum was investigated by Reier and Shamos[9] and by Braid[10] using a single-crystal scintillation spectrometer and a two-crystal Compton spectrometer. Although Cr^{53} is 9.55% abundant in the natural element, the neutron-capture gamma yield[2] is 55.9% owing to the 17.5-b Cr^{53} cross section. Ambiguities, nevertheless, arise in the assignment of the correct gammas from among the four capturing isotopes.

Trumpy[11] has made an angular correlation measurement on the 8.88–0.84-MeV cascade in natural chromium, finding the capture state to be purely 1^-. A measurement of the circular polarization of the 8.88- and 9.72-MeV gammas arising from capture of polarized

* Work done under the auspices of the U. S. Atomic Energy Commission.

[1] A. W. Schardt and B. J. Dropesky, Bull. Am. Phys. Soc. **1**, 162 (1956).

[2] *Nuclear Data Sheets*, compiled by K. Way *et al.* (Printing and Publishing Office, National Academy of Sciences–National Research Council, Washington 25, D. C., 1961).

[3] D. S. Andreyev, A. P. Grinberg, G. M. Gusinskii, K. I. Erokhina, and I. Kh. Lemberg, Izv. Akad. Nauk S.S.S.R., Ser. Fiz. **24**, 1474 (1960) [translation: Bull. Acad. Sci. U.S.S.R. Phys. Ser. **24**, 1466 (1961)].

[4] W. C. Porter, D. M. Van Patter, M. A. Rothman, and C. E. Mandeville, Phys. Rev. **112**, 468 (1958).

[5] A. J. Elwyn and F. B. Shull, Phys. Rev. **111**, 925 (1958).

[6] F. A. El Bedewi and S. Tadros, Nucl. Phys. **19**, 604 (1960).

[7] B. B. Kinsey and G. A. Bartholomew, Phys. Rev. **89**, 375 (1953).

[8] L. V. Groshev, A. M. Demidov, V. N. Lutsenke, and V. I. Pelekhov, *Atlas of γ-ray Spectra from Radioactive Capture of Thermal Neutrons*, translated by J. B. Sykes (Pergamon Press, Inc., New York, 1959).

[9] M. Reier and M. H. Shamos, Phys. Rev. **100**, 1302 (1955).

[10] T. H. Braid, Phys. Rev. **102**, 1109 (1956).

[11] G. Trumpy, JENER Publ. **No. 13** (1957); Nucl. Phys. **2**, 664 (1956).

TABLE I. Chromium-54 capture-gamma energies and intensities. Gammas taken from natural chromium studies are limited to those assigned by the author to Cr^{54}. Intensities are given in gammas per 100 captures in pure Cr^{54}. Last digit errors are put in parentheses. Results of the present work are included for comparison. Asterisk indicates agreement with Kinsey and Bartholomew.

Kinsey and Bartholomew		Groshev *et al.*		Braid		Kane *et al.*	Present work		
E(MeV)	I	E(MeV)	I	E(MeV)	I	E(MeV)	E(MeV)	I(rel)	I(abs)[a]
9.716 (7)	13	9.72 (2)	13			*	*	(*)	20
8.881 (7)	34	8.88 (2)	36			*	*	(*)	56
7.097 (6)	4.6	7.09 (2)	6.1			*	*	(*)	6.5
6.872 (8)	1.1	6.88 (3)	1.8			*	*	(*)	1.9
6.644 (6)	5.4	6.65 (2)	7.5			*	*	(*)	7.0
6.26 (2)	1.6	...	...			6.31	*	(*)	2.4
6.00 (1)	1.8	6.00 (3)	2.9			5.97	*	(*)	1.7
...	...	4.90 (3)	2.4			~4.9(?)			0.5
							4.86 (3)	0.3 (1)	
4.83 (1)	1.1	4.80 (3)	1.1			4.83			2.1
3.72 (2)	0.9	3.70 (2)	2.4			*	*	0.20 (4)	1.7
		...	...			2.56	2.60 (2)	0.29 (6)	2.4
		2.32 (2)	3.5	2.28 (3)	18	2.22	2.24 (1)	1.00	8.5[b]
		...	...			...	2.00 (2)	0.22 (4)	1.9
		1.75 (2)	3.5	1.84 (3)	11	1.78	1.77 (1)	0.94 (6)	8.0[b]
		0.840 (15)	36	0.83	71	0.84	0.84 (1)	9.1 (9)	78

[a] See text, Sec. IV.
[b] May include up to 20% additional intensity from a secondary transition (see text Sec. IV).

neutrons showed both transitions to be electric dipole.

Kane, Fiebiger, and Fox[12] have recently made a definitive capture-gamma study of the chromium isotopes, using natural chromium and two enriched isotopes. They used a three-crystal pair spectrometer and a single crystal to study, respectively, the high- and low-energy spectrum, both singly and in coincidence. They propose energy levels at 0.84, 2.62, 2.84, 3.07, 3.41, 3.72, and 4.89 MeV.

Capture gammas attributed to Cr^{54} as a result of the present study, as well as the previous studies, are summarized in Table I.

II. EXPERIMENTAL APPARATUS

A. Thermal Neutron Beam

Target size and detector geometry conditions indicated that a flux of (1 to 5)$\times 10^6$ thermal neutrons/cm^2 sec was needed to achieve a singles counting rate of 10^4/sec. We planned to use a 6-in.-diam beam port which looked at the core of the Livermore 2-MW pool type reactor.

In order to remove the sizable fast neutron and gamma contamination, we considered (a) a moderating medium at the front end of the beam tube; (b) a diffracted beam using a monochromating crystal[13]; (c) a beryllium "cold" neutron filter[14]; and (d) a quartz crystal filter.[15] The moderating medium was easily shown to be unfeasible due to the small diameter of the beam tube. The monochromating crystal method makes inefficient use (1–3%) of the thermal neutron spectrum, although with some effort it could have been useful.

Absorbing or scattering transmission filters must be designed so that their crystalline properties are exploited, since free-atom cross sections are always larger for thermal than for fast neutrons. A cold neutron filter utilizes a microcrystalline material, and exploits the fact that a perfect lattice will not scatter neutrons of wavelength longer than the largest Bragg spacing. Metallic beryllium, the best material for this purpose, efficiently transmits only about 1% of a 300°C Maxwell thermal distribution ($E<0.005$ eV). Moreover, it was found that over 30 cm of beryllium was needed to attenuate the gamma contamination to a usable level. Since thermal diffuse scattering in the beryllium [$\tau(300°\text{C})=0.069$ cm^{-1}] further attenuated the cold flux, it was concluded that a useful beam would be feasible only by cooling the beryllium to liquid-nitrogen temperature [$\tau(180°\text{C})=0.0075$ cm^{-1}].

A "single-crystal" thermal neutron filter exploits the fact that coherent scattering in a perfect lattice is restricted to wavelengths which satisfy the Bragg relation. Requisite criteria are low-capture and incoherent scattering cross sections, small mosaic spread, and high Debye temperature.

The absorption coefficient of quartz at room temperature is 0.055 cm^{-1} for thermal neutrons, increasing to 0.2 cm^{-1} for fast neutrons. Although cooling with liquid nitrogen would greatly enhance the thermal neutron transmission [$\tau(180°\text{C})=0.020$ cm^{-1}], it was clear that 50–75 cm of crystalline quartz would yield a sufficiently clean 10^6/cm^2 sec thermal beam at room temperature.

Neutron transmission measurements were made on 20 large (~0.3 kg) but highly imperfect quartz crystals. In most cases we found the attenuation to be consistent

[12] W. R. Kane, N. F. Fiebiger, and J. D. Fox, Phys. Rev. **125**, 2037 (1962).
[13] G. Manning and G. A. Bartholomew, Phys. Rev. **115**, 401 (1959).
[14] P. A. Egelstaff and R. S. Pease, J. Sci. Instr. **31**, 207 (1954).
[15] B. N. Brockhouse, Rev. Sci. Instr. **30**, 136 (1959).

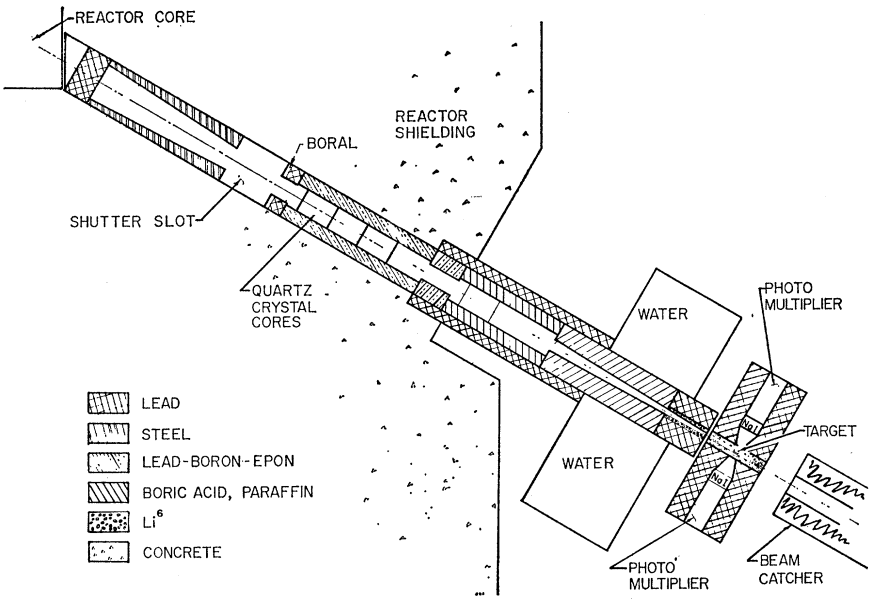

FIG. 1. Schematic of thermal neutron filter and experimental geometry.

with diffuse scattering alone, and independent of crystal orientation. Several selected crystals were cored and faced to 6.35-cm diam by 12–18 cm long. Five of these cores were inserted in a section of the tapered collimator (Fig. 1), and 15 cm of lead was inserted in the reactor end of the collimator to attenuate core gammas.

The thermal flux at the target was calibrated with a BF_3 counter and found to be $1.2\times10^6/cm^2$ sec with a cadmium ratio of 20 000 (0.089 cm Cd). Moreover, most of the neutron contamination was found to be from the epithermal region.

B. Target and Detectors

A 0.292-g sample of Cr^{53}-enriched Cr_2O_3 was obtained.[16] The quoted enrichment was 95.3%, corresponding to a 99.7% capture yield. Spectroscopic analysis of possible impurities indicated negligible contamination of the capture gamma spectrum. The sample was encapsulated in a thin-wall cylinder of CD_2 (deuterated polyethylene).

The target was looked at by two 2-in. $\times$2-in. NaI(Tl) crystals, each mounted on an RCA 6655-A PM tube. The target and detector were surrounded by a lead shield (Fig. 2). The neutron beam, collimated to 1.2-cm diam, entered and left the shield through a 1.91-cm-i.d. $\times$0.16-cm-thick cylindrical shell of lithium 6 canned in 10-mil aluminum. The target capsule is retained in a CD_2 holder at the center of the tube so that only target material and CD_2 are in the direct beam. The Li^6 prevents scattered neutrons below 10 eV from reaching the detector, but transmits essentially all gammas above 0.03 MeV.

[16] Isotopes Division, Union Carbide Nuclear Company, Oak Ridge, Tennessee.

C. Electronics and Counting Calibration

The spectrometer is based on the fast-slow coincidence system built and used by Schwäger.[17] Figure 3 is a block diagram of the system with the modification used in the "double-window" coincidence technique described in the next section.

With the detector 5 cm from the target axis, the singles counting rate was 0.2×10^4/sec and summing in either crystal was less than 2%. The slow pulses were clipped to about 1.5 μ sec, limiting pileup to less than 0.5%. Background consisted of the ever-present 0.511-MeV positron annihilation gamma superimposed on a continuum which rapidly decreased with increasing energy, becoming negligible above 8 MeV. Its composition, in order of decreasing importance, was (a) reactor-produced room background; (b) beam gammas

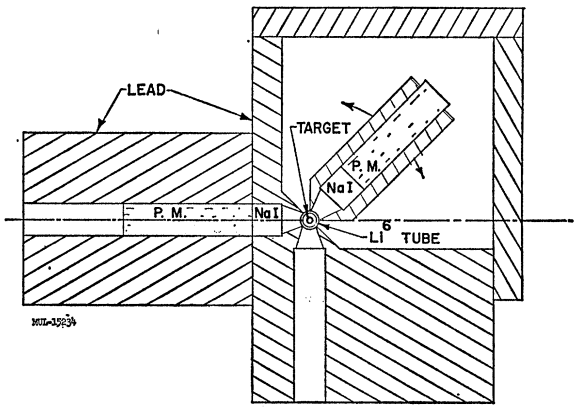

FIG. 2. Angular correlation assembly.

[17] J. E. Schwäger, Phys. Rev. **121**, 562 (1961).

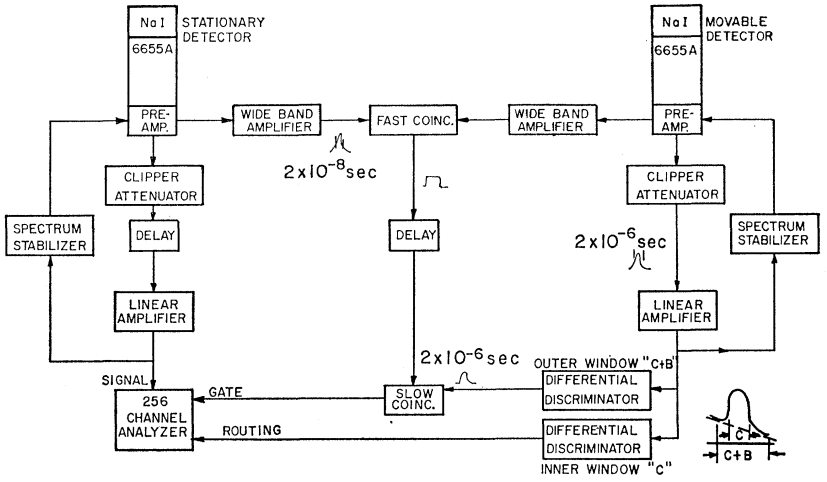

FIG. 3. Block diagram of the spectrometer modified for operation in the "double-window" coincidence mode.

Compton scattered in the target and holder; (c) background produced in the collimator and reaching the detector by devious routes. Cosmic rays and lead or aluminum capture gammas were negligible.

The spectrum of a monochromatic gamma was typically a full-energy photopeak with a Compton tail, a broad backscatter peak at about 0.2 MeV, and a 0.075-MeV lead x-ray peak. Above 1 MeV, the spectrum becomes increasingly dominated by the pair escape peaks at 0.51 and 1.02 MeV below the full-energy peak.

For all coincidence runs, the neutron filter was reduced to 50 cm of quartz, raising the singles rate to about 10^4 per sec and the total fast-coincidence rate to about 300 per sec. The accidental coincident rate was about 2% with a fast resolving time of 30 nsec. Although the singles background ratio and pileup were worsened, the coincident background was less than 2%. Even this is removed in a "double-window" run.

In most of the runs, the spectrum was stabilized with a voltage feedback system[18] built by Schwäger.

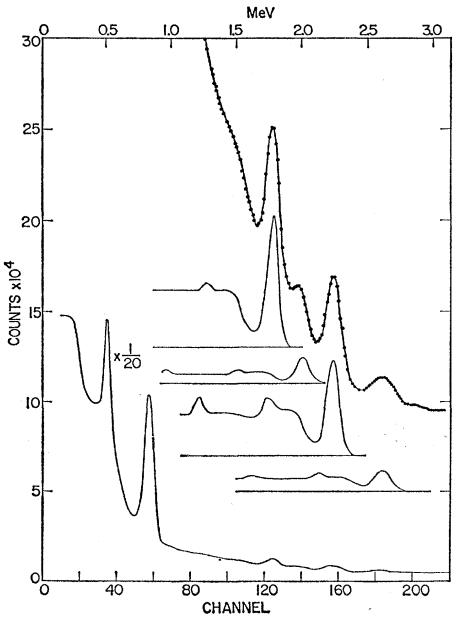

FIG. 4. Low-energy chromium-54 singles spectrum.

D. "Double-Window" Coincidence Technique

The "background" under the peak in the gating branch of the coincidence system consists essentially of nontarget background previously described, and Compton tails, etc., of higher energy gammas.

In order to systematically correct for the background coincident spectrum, it was decided to accumulate background coincident and peak-coincident spectra simultaneously. A discriminator window C, and a second window (called $C+B$) of width $2C$, are centered on the desired peak (see Fig. 3). The outer window gates the 256-channel analyzer in the coincidence mode and the inner window routes the coincident pulse into the upper half of the analyzer memory. Thus, the C coincident spectrum is accumulated in the lower memory and the B coincident spectrum in the upper. If the background is known to be linear in the region of the peak, the difference of the two coincident spectra is attributed to the desired peak alone. The statistically optimum window width C is roughly given by $(1.07+0.08p/b)w$ where p and w are the peak height above background and the full width at half-maximum, respectively, and b is the background height.

The width and centering of the outer window may be altered to accommodate nonlinear backgrounds, etc., a remaining condition being that the pertinent peak vanishes in the subtracted coincident spectrum. Both windows are counted during the run to guard against electronic drifts.

This method is particularly useful for angular correlation measurements since it is independent of beam

[18] A. M. Hoogenboom, Nucl. Instr. 3, 57 (1958).

intensity fluctuations where runs are normalized to singles counts in channel C. Other advantages include equalized dead-time losses. halved running time, and background taken most representative of that at the peak.

III. EXPERIMENTAL RESULTS

A. Singles Spectra

The Cr^{54} singles spectrum was accumulated with detector 1, which had 7.9% resolution for the 0.662-MeV Cs^{137} peak. The low-energy spectrum (Fig. 4) was found to contain peaks at 0.84±0.01, 1.77±0.01, 2.24±0.01, and 2.60±0.02 MeV, in addition to annihilation radiation (0.51 MeV), and the possibility of a peak at 2 MeV. No peaks were seen below 0.5 MeV. The region from 1.5 to 3.0 MeV was analyzed using spectra interpolated from those of Na^{24} β-decay gammas and the hydrogen capture gamma, produced under identical conditions. At 2.00±0.02 MeV a gamma is clearly present. The relative intensities were evaluated (Table I) from the photopeak areas, knowing the calculated total crystal efficiency and photoefficiency.

TABLE II. Sum coincident cascades.

Cascade (MeV)	Relative intensity
8.88–0.84	23 (4)
8.45–1.27	<0.08
7.10–2.61	<0.05
6.88–2.84	<0.08
6.64–3.08	<0.08
6.28–3.44	<0.08
6.00–3.72	1.00
4.86–4.86	0.25 (5)

The higher energy portion of the spectrum (Fig. 5) is complicated by the enhancement of the escape peaks. Although accurate intensity assignments could not be made, the spectrum was accounted for in terms of gammas at 3.72, 4.86, 6.00, 6.28, 6.64, 6.88, 7.10, 8.88, and 9.72 MeV, appropriately taken from the natural chromium spectrum seen by KB (Ref. 7) and GDLP (Ref. 8).

B. Sum Coincidence Spectrum

Single-stopover transitions from the capture to ground state were studied by sum coincidence.[18] The detector axes were oriented to subtend a 90° angle at the target. The lead shielding between them prevented false coincidences resulting from a single gamma scattering from one crystal into the other. The analyzer was fed by detector 1, but was gated only when a fast coincidence occurred, and when the pulses in the two detectors summed to a height which fell in a discriminator window [Fig. 6(a)] centered on 9.72 MeV, the neutron binding energy.

Although the counting rate was low, the spectrum [Fig. 6(b)] clearly shows the transitions 8.88–0.84,

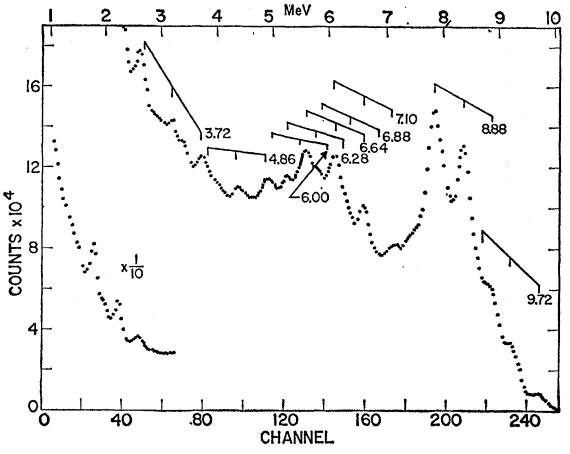

FIG. 5. High-energy chromium-54 singles spectrum. Bars indicate position of the full-energy peak and the two escape peaks associated with each gamma.

6.00–3.72, and 4.86–4.86 MeV. The branching ratios of these cascades, and limits on other possible cascades, were determined (Table II).

Lowering the sum window enhanced the counting rate, but complicated the spectrum considerably [Fig. 6(c)] since two-step cascades to the 0.84-MeV level were then allowed.

C. Coincidence Measurements

A spectrum was first taken in coincidence with the 0.84-MeV peak (Fig. 7). Peaks at 3.72, 6.00, and 9.72 were clearly absent. All other peaks were present in roughly the amount seen in the singles spectrum.

Coincidence spectra were taken with the 1.77, 2.00, 2.24, and 2.60 peaks. All cases (Table III) are consistent with a two-step cascade from the capture to the 0.84-MeV level.

An intensive search was made for the populating of the level at 1.27 MeV, proposed as a result of (d,p) work. If this level were populated at all, it must decay

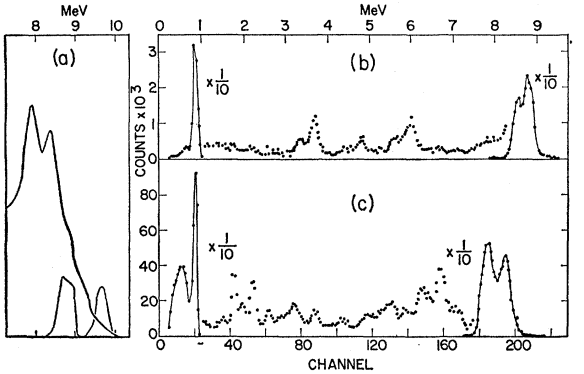

FIG. 6. Chromium-54 sum coincident spectrum: (a) gating spectrum and window response; (b) sum spectrum coincident with the upper window; (c) sum spectrum coincident with the lower window.

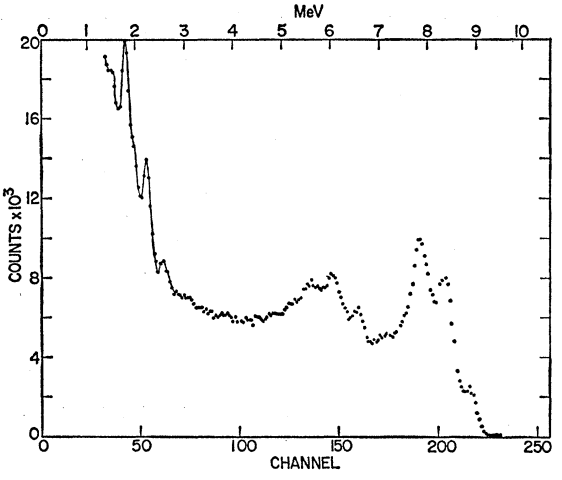

FIG. 7. Chromium-54 spectrum coincident with the 0.84-MeV peak.

by either a 1.27-MeV transition, or a 0.43–0.84-MeV cascade. No evidence for either was found in the singles spectrum.

Coincidence measurements were made by observing the 8-MeV region with a window around 0.5 MeV. Alternatively, the low-energy region was observed with a window around 7.7 MeV (Fig. 8). It was concluded that the intensity of transitions to or from a 1.27-MeV level is less than 10^{-2} with respect to the 8.88–0.84-ground cascade.

In order to determine the branching modes of decay from the 4.86 level, a coincidence window was set in the region of the 4.86-MeV photopeak and first escape peak. The coincident spectrum (Fig. 9) shows the presence of a second 4.86-MeV gamma, expected from sum coincidence results. The analysis of the 4-MeV region is complicated by the presence of the 3.72-MeV gamma, resulting from coincidence with the Compton tail of the 6.00-MeV gamma. The intensity of any 4.02-MeV gamma, respresenting a transition from the 4.86- to the 0.84-MeV level, is found to be less than 0.2 with respect to the 4.86 peak.

D. Angular Correlation Measurements

The ground and first excited states of Cr^{54} are known to have spins and parities 0^+ and 2^+, respectively.[2] It was decided that the spins of the 2.62-, 2.84-, 3.08-,

TABLE III. High-energy peaks in coincidence with peaks in the 2-MeV region.

Energy of coincidence window (MeV)	Highest coincident peak (MeV)	Relative intensity limit for higher energy peaks
1.77	7.10	0.03
2.00	~6.9	0.10
2.24	6.64	0.03
2.60	~6.3	0.05

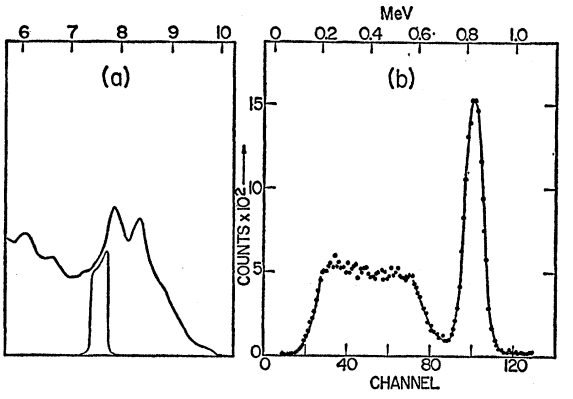

FIG. 8. Chromium-54 spectrum in coincidence with the 7.5-MeV region: (a) gating spectrum and window response; (b) singles and coincident spectrum.

and 3.44-MeV levels could be measured by direction correlation using the 0.84-MeV gamma as part of a two-step cascade. The angular correlation would then be given by

$$W(\theta)=A_0+A_2P_2(\cos\theta)+A_4P_4(\cos\theta),$$

where the P's are the Legendre polynomials, and the angular distribution function is normalized so that $A_0=1$.

In an effort to optimize the statistics, measurement was restricted to 90°, 135°, and 180°.[19] The double window was set on the 0.84-MeV peak and a spectrum at each angle was taken for 10^6 counts in the inner window. We also counted the outer window to guard against drift effects.

The detectors were repeatedly cycled through the three angles, taking a total of 23 runs at each angle. Each run took about 36 min. The upper and lower analyzer memories were printed out after each run, and their difference was taken. All difference spectra taken

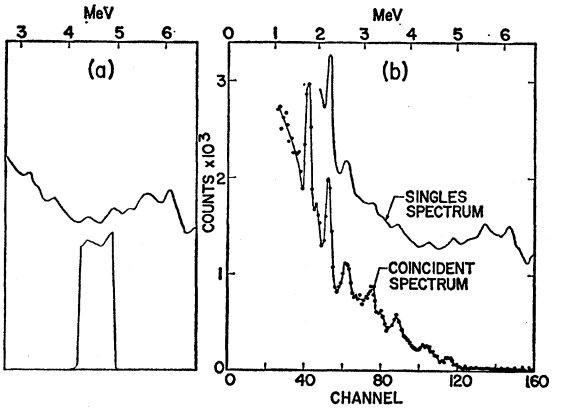

FIG. 9. Chromium-54 spectrum in coincidence with the 4.86-MeV region: (a) gating spectrum and window response; (b) singles and coincident spectrum.

[19] D. H. White, Nucl. Instr. **21**, 209 (1963).

TABLE IV. Corrected angular correlation coefficient and compatible spins corresponding to cascades from the pertinent state to the ground state (0^+) via the 0.84-MeV (2^+) level.

Level energy (MeV)	Cascade (MeV)	A_2	A_4	Nuclear spin
2.61	1.77–0.84	0.500±0.030	0.008±0.060	2
2.84	2.00–0.84	0.299±0.110	1.107±0.220	0
3.08	2.24–0.84	0.178±0.030	0.073±0.068	2,3
3.44	2.60–0.84	0.182±0.080	−0.035±0.180	1,2,3
9.72	8.88–0.84	−0.252±0.006	−0.007±0.015	1

at each angle were then added (Fig. 10). Analysis was difficult due to the overlap of the four gamma spectra.

The 8.88–0.84-MeV cascade of Cr^{54} was also measured with the double window on the 0.84 peak as before. Twelve runs were taken for about 50 min per run. An angular correlation was run with the well-known cobalt-60 cascade, as a check against possible systematic error.

Explicit expressions were evaluated for all corrections pertinent to finite target and detector dimensions and masses.[19] Since the target was quite small, only the corrections for finite target length and detector aperture were important. These effects attenuate the correlation coefficients A_2 and A_4 by 0.810 and 0.490, respectively, in the case of the 1.77–0.84-MeV cascade, for example.

The corrected coefficients are referred to a plot[20] of A_2 versus A_4 (Fig. 11) in which loci of points are given for the possible spin combinations.

The results are summarized in Table IV.

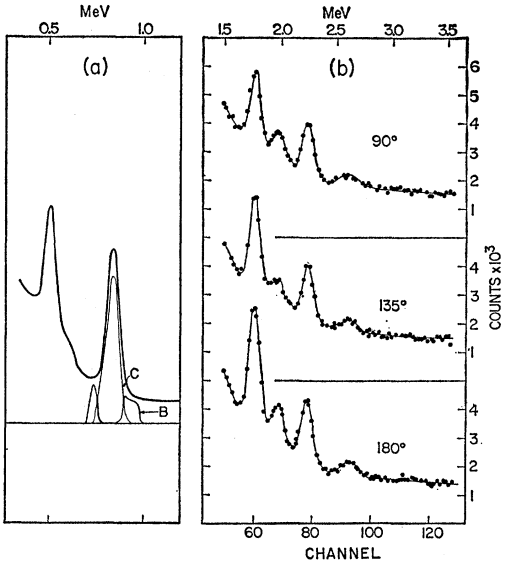

FIG. 10. Chromium-54 spectra for 0.84-MeV coincident angular correlation: (a) gating spectrum and double-window response (detector 1); (b) subtracted coincident spectra (detector 2).

IV. DISCUSSION

The energy level scheme of Cr^{54} is shown in Fig. 12. The levels at 0.84, 1.27, 2.62, 3.08, and 3.72 MeV were taken from the (d,p) measurements,[5,6] readjusted to fit the more accurate capture-gamma energies. The $l=1$ character of the angular distributions identifies all the levels with positive parity. The levels at 2.84 and 3.44

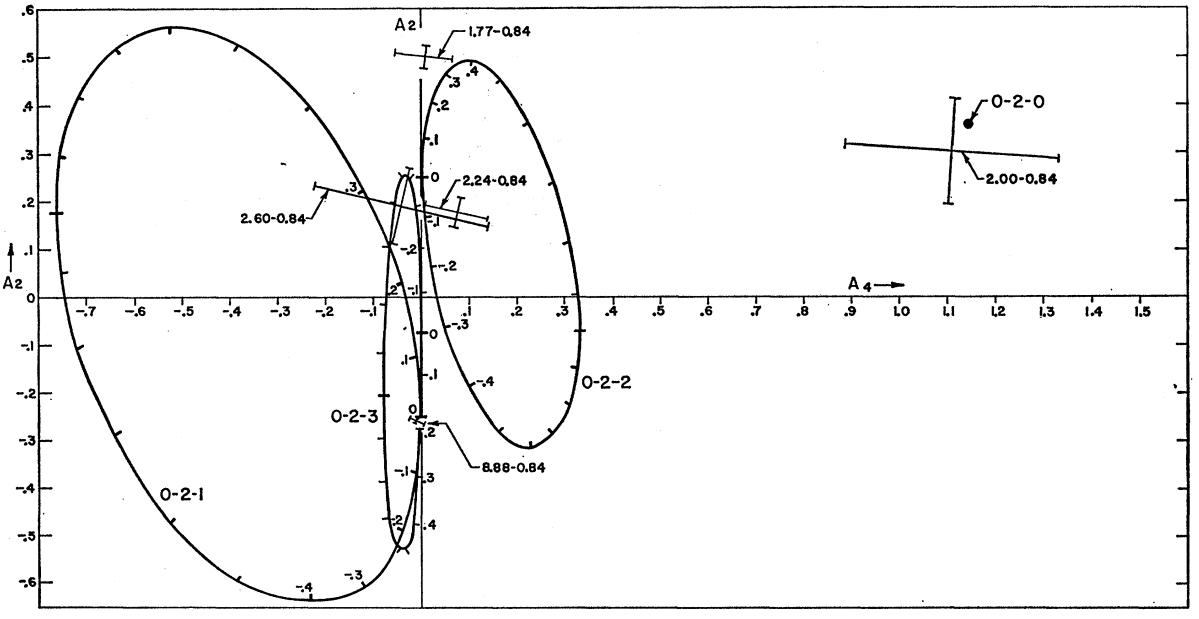

FIG. 11. Plot of A_2 versus A_4 for possible cascade combinations. The parameter $\delta'=\delta(1+|\delta|)^{-1}$ is shown, where δ^2 represents the quadrupole-to-dipole mixing ratio. Data points are shown with statistical errors only. Axes are oriented to conform to statistical independence (see Refs. 19 and 20).

[20] C. F. Coleman, Nucl. Phys. 5, 495 (1958).

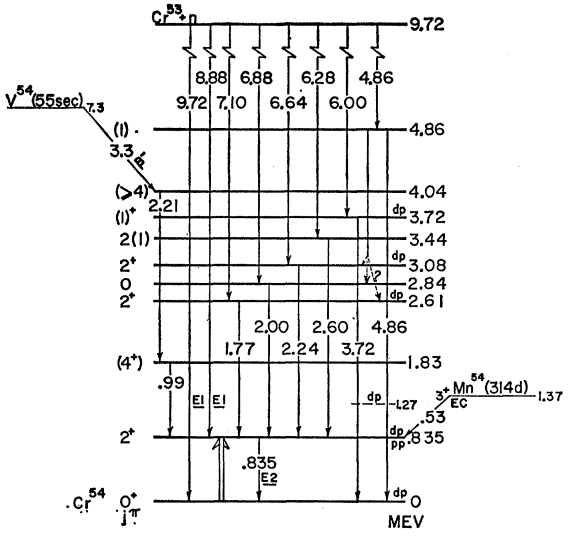

FIG. 12. Chromium-54 energy level scheme.

MeV were established as a result of the present work and that of Kane *et al.* Since these levels are both deduced only by the two-step cascades to the 0.84-MeV level, the unlikely possibility exists that the stated transition orders of either could be inverted.

The 3.72 level is seen to decay only to the ground state with less than 12% to any other proposed level. The 2.61, 2.84, 3.08, and 3.44 levels are seen to decay only to the 0.84 level. The upper limits of the possible crossover ground-state branching ratio for these levels are 0.02, 0.04, 0.02, and 0.04, respectively, as determined by sum coincidence.

It is noted that KB find gammas at 6.26 and 6.36 MeV with intensities (normalized to pure Cr^{54} capture) of 1.6 and 0.5, respectively. However, GDLP find a 6.35-MeV gamma with intensity 1.4, but no 6.26 gamma. Kane *et al.* propose a level at 3.41 deduced from coincident gammas at 2.56 and 6.31 MeV. The latter was taken to contribute in part to the GDLP 6.36-MeV peak in natural chromium. We find coincident gammas at 2.60±0.02 and 6.27±0.04 MeV, in agreement with the 6.26-MeV gamma of KB. The 2.60 coincidence and the sum coincidence results attribute the 2.60-MeV gamma only to the 3.45–0.84-MeV transition, with an upper limit of 4% to the ground-state deexcitation of the 2.61-MeV level suspected by Kane *et al.*

A 4.86-MeV doublet was seen in our sum coincidence measurements. GDLP had found 4.80- and 4.90-MeV gammas, the latter having greater intensity. However, KB and Kane *et al.* found a peak at 4.83 MeV, but little evidence of another nearby peak. We were unable to resolve the two gammas, and consider them separated by less than 0.06 MeV. Moreover, the composite peak (Figs. 5 and 9) appears closer to 4.86 than 4.83, in spite of the unequal gamma intensities.

By comparing the sum coincident intensity with the singles spectrum, the direction ground-state decay of the 4.86 level accounts for only about 20% of its population. Also, the 0.84-MeV coincidence showed the majority of the 4.86-MeV gammas were involved with a cascade to the 0.84-MeV level. A direct 4.86-to-0.84-MeV transition cannot account for the missing link, since no 4.02-MeV gamma was found either in the singles or the 4.86 coincident spectrum.

The 4.86-MeV level could, however, decay to either the 2.61- or 3.08-MeV level, or both. These alternatives cannot be distinguished since the de-excitation energy to either level is within 0.01 MeV of the de-excitation energy from the other, and the gammas would be hidden. This contribution to the 1.77- or 2.24-MeV peaks would be only about 20% at most.

A similar argument may be made concerning the 2.84 level, although the intensity of the 2.00-MeV gamma could account for only a fraction of the missing 4.02-MeV cascade.

It must be realized that the angular correlation analysis may contain systematic errors due to the possible contamination of the 1.77-, 2.00-, and 2.24-MeV gammas. However, the contamination is small and should not affect the spin assignments.

No evidence is found for the 1.27-MeV level deduced from the (d,p) work. Population from the capture state is less than 0.006 per capture as seen from coincidence and sum coincidence measurements. Population by a more devious route is less than 0.01 per capture as seen from a study of the low-energy singles spectrum. It is difficult to explain the (d,p) results. Only a state of spin 3 would be expected to be populated by an $l=1$ stripping process but not by de-excitation of the 1^- capture state. On the other hand, a spin-3 state should be populated by the higher spin-2 states.

With the exception of the 4.86-MeV gamma, the energies found in our work are compatible within errors with the energies and energy differences of KB. A consistent set of gamma energies and energy levels (Fig. 12) are determined.

The absolute gamma intensities may be uniquely determined from our relative intensities (Table I) and the 9.72–8.88-MeV gamma intensity ratio of 0.36 taken from KB and GDLP. It is also assumed that the proposed scheme is both correct and complete, with respect to capture gamma processes. Agreement is generally good considering the wide variations among other experiments. These values are considerably higher than KB and GDLP for the two highest energy gammas. However, it would be difficult to explain this discrepancy unless about 30% of the capture-state transitions remained unseen.

The capture state must have a spin of 1^- or 2^- since the measured Cr^{53} ground-state spin is $\frac{3}{2}^-$. The angular correlation measurements show that the 8.88–0.84 cascade is consistent with a pure $1^-(E1)2^+(E2)0^+$ transition, as Trumpy[11] has already demonstrated. Assuming only $E1$ transitions from the capture state, the precision of the measurement limits the 2^--to-1^- capture ratio to

less than 0.02, at least as far as the transition to the 0.84-MeV level is concerned.

The 1.77–0.84-MeV angular correlation unambiguously shows the cascade to be $2^+(M1,E2)2^+(E2)0^+$ with quadrupole mixing parameter $\delta=0.47\pm0.05$. The parity assignment of the 2.62-MeV level is consistent with the fact that $E1$ and $M2$ mixing would be extremely unlikely in the amount observed, and with the $l=1$ stripping results. The 2.84 level clearly has spin 0.

Both the 3.08- and 3.44-MeV levels are consistent with spin 2 and with de-excitation quadrupole mixing parameter $\delta=-0.08\pm0.04$ and $\delta=-0.09\pm0.11$, respectively. Although spin 3 cannot be ruled out, it would be possible only if either the population occurs via a quadrupole transition from the capture state, or a dipole transition from a 2^- capture state. Quadrupole transitions are extremely unprobable, being about $10^{-3}(3^+)$ to $10^{-5}(3^-)$ with respect to electric dipole transition, according to single-particle estimates. Capture into a 2^- state cannot be dismissed as lightly, although one would have expected measurable $E1$ decay of such a state to the 0.84-MeV level. Spin 1 for the 3.44-MeV level cannot be ruled out, although absence of dipole decay to the ground state makes this unlikely.

The 3.72 and 4.86 levels are most probably spin 1, since no other possibilities are reasonably consistent with decay to the ground (0^+) state but not to the first excited (2^+) state.

Parities cannot be assigned to the 4.86-, 3.44-, and 2.84-MeV levels, although positive parity is likely, since $M1$ transitions would compete poorly with $E1$ transitions from the capture state. On the other hand, negative parity is suggested due to the conspicuous absence of $l=1(d,p)$ peaks, and in the 3.44-MeV case, absence of quadrupole transitions to the ground and first excited states.

The 1.82-MeV level, populated by vanadium-54 β^- decay,[1] undoubtedly has spin greater than 3, since it is not populated from the capture state or the other higher levels. The 4.04-MeV level must also have spin greater than 3 to account for its decay.

CONCLUSIONS

Noteworthy results for Cr^{54} include: (a) lack of $E2$ ground-state transitions from the $2'$ and $2''$ states (2.61 and 3.08 MeV, respectively); (b) $E2/M1$ ratio for the $2'$(2.61 MeV) $\rightarrow 2$(0.84 MeV) transition enhanced (0.23) with respect to shell-model estimates[21] (0.002); and (c) relatively large energy spacing between the first four levels. Coulomb excitation studies[3] indicate that the $2\rightarrow 0$ $E2$ transition is enhanced by about 10 over single-particle estimates.

These features seem generally to fit a pattern noted by others.[22–24] For even-even nuclei, the ground state is always 0^+, and the first excited state is almost always 2^+. Van Patter[22] noted that the spin of the second excited state is 4^+ for $22\leq N\leq 30$. On the other hand, the region $32\leq N\leq 88$ (called the "vibration" region) is characterized by a second excited state of 2^+. The energy ratio $E_{2'}/E_2$ drops sharply below 2 for $32\leq N<40$, and ranges from 2 to 2.5 for $40\leq N\leq 88$. The $2'\rightarrow 0$ $E2$ crossover transition is severely inhibited (a few percent) with respect to the $2'\rightarrow 2$ transition. The latter proceeds by $E2$ with a small ($\sim 10\%$) mixture of $M1$.

Above $N=90$, the level sequence changes abruptly to 0^+, 2^+, 4^+, $\cdots$, displaying rotational character. On the other hand, light nuclei have been found[25] ($N\approx 10$) whose spectra can be interpreted in terms of rotational states as well as by the shell model. Chromium-54 lies in a transition region in which both independent particle interactions and collective effects may be important. It is reasonable, therefore, to review nuclear models applicable to the vicinity of Cr^{54}.

An asymmetric rotor theory (hydrodynamical model) has been proposed by Davydov and Filippov,[26] resulting from intermediate coupling to the core.[27] The model gives specific predictions concerning the energy ratio $E_{2'}/E_2$ and corresponding reduced $E2$ transition probabilities in terms of the ellipsoidal deformation parameter γ. Van Patter[28] finds an excellent fit of these relations to nuclei for $N>40$. The sudden appearance of collective effects at $N=32$ was found to be quite striking. The value $E_{2'}/E_2=3.125$ for Cr^{54} is consistent with $\gamma=21.7°$. However, the corresponding $2'\rightarrow 0/2'\rightarrow 2$ branching ratio is 0.130, whereas the experimental value is less than 0.012. Moreover the 4^+ level is predicted at about 2.6 MeV. Mallman[29] has introduced rotation-vibration interaction as a perturbation to the generalized quasiadiabatic asymmetric rotor theory, and shows an agreement in low-lying even parity states in non-closed-shell nuclei with $40\leq A\leq 250$. However, Cr^{54} is underdetermined since four energy levels are needed in the ground-state band (0^+ state is not included) to determine the model parameters. The model is expected to break down in the vicinity of closed shells (Cr^{52}, for example).

The collective model of Bohr and Mottelson[30] has been studied by Wilets and Jean[31] in terms of strong

[21] G. Scharff-Goldhaber, in *Proceedings of the University of Pittsburgh Conference on Nuclear Structure, 1957*, edited by S. Meshkov (University of Pittsburgh and Office of Ordnance Research, U. S. Army, 1957), p. 447.

[22] D. M. Van Patter, Bull. Am. Phys. Soc. **3**, 212 (1958).

[23] G. Scharff-Goldhaber and J. Weneser, Phys. Rev. **98**, 212 (1955).

[24] K. Alder, A. Bohr, T. Huus, B. Mottelson, and A. Winther, Rev. Mod. Phys. **28**, 432 (1956).

[25] S. Moszkowski, in *Proceedings of the University of Pittsburgh Conference on Nuclear Structure, 1957*, edited by S. Meshkov (University of Pittsburgh and Office of Ordnance Research, U. S. Army, 1957), p. 508.

[26] A. Davydov and G. Filippov, Nucl. Phys. **8**, 237 (1958).

[27] A. Davydov and G. Filippov, Nucl. Phys. **10**, 654 (1959).

[28] D. M. Van Patter, Nucl. Phys. **14**, 42 (1959).

[29] C. A. Mallman, Nucl. Phys. **24**, 535 (1961).

[30] A. Bohr and B. Mottelson, Kgl. Danske Videnskab. Selskab, Mat. Fys. Medd. **27**, No. 16 (1953).

[31] L. Wilets and M. Jean, Phys. Rev. **102**, 788 (1956).

coupling to quadrupole surface oscillations (adiabatic approximation). They find that γ instability leads to a single-phonon-transition selection rule forbidding the $2' \rightarrow 0$ crossover transition, and enhanced $2' \rightarrow 2$ and $2 \rightarrow 0$ $E2$ transitions. However, the predicted two-phonon second excited state is a degenerate triplet (0^+, 2^+, 4^+) with an energy twice the one-phonon first excited state. The degeneracy can be lifted to some extent by deforming the potential, but the observed energy ratios ($E_{2'}/E_2=3.13$ and $E_4/E_2=1.83$) cannot adequately be explained. Moreover, the strong coupling approximation is not expected to be valid in the region of Cr^{54} where individual particle interactions are known to play an important role.

Scharff-Goldhaber and Weneser[23,21] have considered the weak coupling of individual nucleons $[(f_{7/2})^4]$ to a core with free-surface quadrupole oscillations, in order to explain the systematics for $36<N<88$. Results are generally those of the strong-coupling solution. Again the model cannot adequately account for the energy spacings.

Raz[32] has examined the weak-coupling solution in terms of variable surface coupling added to a variable two-nucleon $(f_{7/2})^2$ interaction. He shows that for moderately weak surface coupling, the multiple phonon components of the low-lying excited states depend vitally upon the strength of the two-nucleon interaction with respect to the surfon energy. Such an approach appears to have considerable promise, provided that the proper independent-particle states are incorporated.

All these modified phonon models are capable of predicting a spin sequence 0^+, 2^+, 4^+, 2^+, 0^+, enhanced $E2$ transitions, and lack of a $2' \rightarrow 0$ crossover transition. However, the large level spacing and the rather modest enhancement of the reduced $E2$ transition amplitudes of Cr^{54} suggest that vibrational modes play only a minor role. Ford and Levinson[33] have pointed out that although coupling to surface oscillations should be considered, it is of negligible importance in determining consistent level spacings for the calcium isotopes.[34] Indeed, Schwarcz[35] has determined the correct sequence and relative spacings of the low-lying levels of Mn^{55} and V^{51} assuming only two-nucleon forces between nucleons outside the closed shells.

In summary; a fairly abrupt systematic change seems to occur between the "shell-model" region below $N=30$ and the "vibrational" region above $N=32$. Chromium-54 appears to be just below the vibrational region in which multiple phonon or rotational effects dominate the level structure. It remains to study the alternative interpretation in terms of the shell model, in which appropriate two-nucleon forces characterize the $(f_{7/2})^4$ and $(p_{3/2})^2$ groups outside the closed core. The large values of δ^2 and the small value of the $2' \rightarrow 0$ transition rate would follow from seniority conditions,[36] and the moderate $E2$ transition enhancement could result from suitable mixing.

ACKNOWLEDGMENTS

I wish to thank Dr. J. E. Schwäger, Comdr., U. S. Navy, for the use of the coincidence spectrometer and for motivating my interest in capture studies. I am also indebted to Dr. Albert Kirschbaum for his support of the program, and to Dr. Terry Crow and Richard Phillips for their help in operation and data analysis.

[32] B. James Raz, Phys. Rev. **114**, 1116 (1959); and private communication.

[33] K. W. Ford and C. Levinson, Phys. Rev. **100**, 1 (1955).

[34] C. Levinson and K. W. Ford, Phys. Rev. **100**, 13 (1955).

[35] E. H. Schwarcz, Phys. Rev. **129**, 727 (1963), and private communication.

[36] J. J. Kraushaar and M. Goldhaber, Phys. Rev. **89**, 1081 (1953).